3′-Deoxy-3′-^{18}F-Fluorothymidine PET–Derived Proliferative Volume Predicts Overall Survival in High-Grade Glioma Patients

Albert J.S. Idema[1], Aswin L. Hoffmann[2,3], Hieronymus D. Boogaarts[1], Esther G.C. Troost[2,3], Pieter Wesseling[4,5], Arend Heerschap[6], Winette T.A. van der Graaf[7], J. Andre Grotenhuis[1], and Wim J.G. Oyen[8]

[1]Department of Neurosurgery, Radboud University Nijmegen Medical Centre, Nijmegen, The Netherlands; [2]Department of Radiation Oncology, Radboud University Nijmegen Medical Centre, Nijmegen, The Netherlands; [3]Department of Radiation Oncology (MAASTRO), GROW School for Oncology and Developmental Biology, Maastricht University Medical Center, Maastricht, The Netherlands; [4]Department of Pathology, Radboud University Nijmegen Medical Centre, Nijmegen, The Netherlands; [5]Department of Pathology, VU University Medical Center, Amsterdam, The Netherlands; [6]Department of Radiology, Radboud University Nijmegen Medical Centre, Nijmegen, The Netherlands; [7]Department of Medical Oncology, Radboud University Nijmegen Medical Centre, Nijmegen, The Netherlands; and [8]Department of Nuclear Medicine, Radboud University Nijmegen Medical Centre, Nijmegen, The Netherlands

3′-deoxy-3′-^{18}F-fluorothymidine (^{18}F-FLT) is a radiopharmaceutical depicting tumor cell proliferation with PET. In malignancies of the lung, breast, head and neck, digestive tract, brain, and other organs, quantitative assessment of ^{18}F-FLT targeting has been shown to correlate with the proliferation marker Ki-67 and with clinical outcome measures such as time to progression and overall survival (OS). The aim of this study was to assess various PET segmentation methods to estimate the proliferative volume (PV) and their prognostic value for OS in patients with suspected high-grade glioma. **Methods:** Twenty-six consecutive patients underwent preoperative ^{18}F-FLT PET/CT and T1-weighted MRI of the brain after contrast application. The maximum standardized uptake value (SUV_{max}) of all tumors was calculated, and 3 different segmentation methods for estimating the PV were used: the 50% isocontour of the SUV_{max} signal for the $PV_{50\%}$, the signal-to-background ratio (SBR) for an adaptive threshold delineation (PV_{SBR}) method, and the iterative background-subtracted relative threshold level (RTL) method to estimate the PV_{RTL}. The prognostic value of the SUV_{max} and the different PVs for OS were assessed. **Results:** Twenty-two patients had glioblastoma multiforme, 2 had anaplastic oligodendroglioma, 1 had anaplastic ependymoma, and 1 had anaplastic astrocytoma. The median OS was 397 d (95% confidence interval, 204–577); 19 patients died during the follow-up period. The PV_{SBR} showed a significantly ($P = 0.002$) better association with OS than did SUV_{max}, PV_{RTL}, and $PV_{50\%}$. Receiver-operating-characteristic analysis resulted in a threshold volume for the PV_{SBR} of 11.4 cm^3, with a sensitivity and specificity of 70% and 83%, respectively, for the prediction of OS. Kaplan–Meier analyses showed a significant discrimination between short and long OS ($P = 0.024$, log rank) for this threshold. **Conclusion:** The PV as determined by ^{18}F-FLT PET is associated with OS in high-grade malignant gliomas. The SBR method yielded the best results to predict short and long OS.

Key Words: PET/CT; ^{18}F-fluorothymidine; FLT; high-grade glioma; overall survival

J Nucl Med 2012; 53:1904–1910
DOI: 10.2967/jnumed.112.105544

Gliomas are relatively uncommon neoplasms. Most gliomas (especially astrocytic, oligodendroglial, and mixed oligoastrocytic tumors) are diffuse tumors, characterized by extensive, diffuse infiltrative growth in the surrounding brain parenchyma. Ependymal tumors are generally more circumscribed. Glioblastoma, the most malignant diffuse astrocytic tumor, is also by far the most frequent glioma. Despite treatment, most patients with a glioblastoma die within 2 y after diagnosis (median survival, 14.6 mo; 2-y survival, 26.5% (*1*)). Standard treatment consists of maximal surgical resection, external-beam radiotherapy (EBRT) to the tumor or resection cavity as characterized by contrast enhancement on MRI, and concurrent and adjuvant chemotherapy in patients younger than 60 y (*1*). The extent of resection together with the age and Karnofsky performance status are important features determining overall survival (OS) (*2–6*). However, the diagnostic work-up of primary glioma still leaves room for improvement. In diffuse infiltrating glioma, contrast enhancement on MRI is not always present and not fully representative of the most malignant parts of the tumor (*7*). Therefore, more advanced imaging techniques are being explored to better guide surgery and radiotherapy.

^{18}F-FDG is the most commonly used radiopharmaceutical for PET of a wide variety of malignancies. However, for brain tumors the specificity of ^{18}F-FDG is low because of the high uptake in the normal brain cortex. The PET tracer 3′-deoxy-3′-^{18}F-fluorothymidine (^{18}F-FLT) specifically

Received Apr. 24, 2012; revision accepted Jul. 2, 2012.
For correspondence or reprints contact: Albert J.S. Idema, Radboud University Nijmegen Medical Centre, Department of Neurosurgery (internal postcode 636), P.O. Box 9101, 6500 HB Nijmegen, The Netherlands.
E-mail: a.idema@nch.umcn.nl
Published online Oct. 17, 2012.

reflects cellular proliferation, lacks any significant uptake in the normal brain, and may thus be more suitable for molecular imaging of gliomas (*8*). Intracellular uptake of ^{18}F-FLT is facilitated both by active transport through sodium-dependent nucleoside transporters and by passive diffusion (*9*). In the cell, ^{18}F-FLT is monophosphorylated by the cytosolic enzyme thymidine kinase 1 and subsequently trapped intracellularly without being incorporated into the DNA (*10*). Because thymidine kinase 1 is upregulated in the S-phase of the cell cycle, ^{18}F-FLT uptake represents the proliferation rate of the tissue. Chen et al. showed that ^{18}F-FLT PET is more sensitive than ^{18}F-FDG PET at detecting recurrent high-grade tumors. The maximum standardized uptake value (SUV_{max}) of ^{18}F-FLT correlated better with the proliferation marker Ki-67 and proved to be a more powerful predictor of tumor progression and survival (*11*). Other investigators confirmed the correlation of ^{18}F-FLT with Ki-67 (*12–14*). However, the relevance of the proliferative volume (PV) of brain tumors as determined with ^{18}F-FLT has not been studied as a prognostic indicator in glioma patients.

In this study, we evaluated the potential of ^{18}F-FLT PET to predict outcome in patients with brain tumors. Because ^{18}F-FLT accumulation is dependent on disruption of the blood–brain barrier (*15*), only patients with suspected high-grade glioma were included in this study. ^{18}F-FLT uptake in the tumors was determined quantitatively, and the PV of brain tumors was estimated using different methods for image segmentation.

MATERIALS AND METHODS

Patients

From July 2007 to August 2008, patients in whom intracranial high-grade glioma was suspected on the basis of a preoperative

TABLE 1
Patient Characteristics

Patient no.	Sex	Operation	Tumor	Prior treatment	Age (y)	Karnofsky score	Deceased	Overall survival (d)	Postoperative therapy
1	M	Resection	Glioblastoma (recurrence)	Surgery, radiotherapy	53	80	Yes	204	Chemotherapy
2	M	Biopsy	Glioblastoma		56	90	Yes	131	Radiotherapy, chemotherapy
3	M	Resection	Glioblastoma		35	90	Yes	602	Radiotherapy, chemotherapy, resurgery, DC
4	M	Resection	ODIII		40	70	No	1,379	Radiotherapy, resurgery
5	M	Resection	Glioblastoma		60	90	Yes	648	Radiotherapy, chemotherapy, resurgery
6	M	Resection	Glioblastoma		45	100	Yes	272	Radiotherapy, chemotherapy
7	F	Biopsy	Glioblastoma		42	90	No	1,349	Radiotherapy, chemotherapy
8	M	Resection	Glioblastoma (recurrence)	Surgery, radiotherapy	36	90	Yes	394	Chemotherapy
9	M	Resection	Glioblastoma		53	80	Yes	155	Radiotherapy
10	F	Resection	Glioblastoma		37	100	No	1,329	Radiotherapy, chemotherapy, resurgery
11	F	Biopsy	Glioblastoma		62	80	Yes	425	Radiotherapy, chemotherapy
12	M	Biopsy	Glioblastoma		66	70	Yes	289	Radiotherapy, chemotherapy
13	F	Resection	Glioblastoma		53	100	No	1,237	Radiotherapy, chemotherapy, resurgery, DC
14	M	Resection	ODIII (recurrence)	Surgery	40	100	No	1,232	Radiotherapy, resurgery
15	M	Resection	Glioblastoma		57	100	Yes	132	Radiotherapy, chemotherapy
16	M	Biopsy	Glioblastoma		59	80	Yes	204	Radiotherapy, chemotherapy
17	M	Resection	Glioblastoma		57	80	Yes	73	No
18	M	Biopsy	Glioblastoma		59	90	Yes	401	Radiotherapy, chemotherapy
19	M	Resection	Glioblastoma		59	100	Yes	227	Radiotherapy, chemotherapy
20	M	Resection	EIII		65	100	Yes	471	Radiotherapy, chemotherapy, resurgery
21	M	Resection	Glioblastoma		49	70	Yes	51	Radiotherapy, chemotherapy
22	F	Resection	Glioblastoma		67	90	Yes	113	Radiotherapy, chemotherapy
23	M	Biopsy	Glioblastoma		64	90	No	1,063	Radiotherapy, chemotherapy
24	M	Biopsy	Glioblastoma		64	70	Yes	185	Radiotherapy, chemotherapy
25	M	Resection	Glioblastoma		48	90	Yes	552	Radiotherapy, chemotherapy, resurgery, DC
26	F	Biopsy	AIII		37	90	Yes	550	Radiotherapy, chemotherapy

DC = dendritic cell therapy.

MRI and in whom surgery was indicated were considered eligible for this prospective study. Exclusion criteria were age younger than 18 y, a Karnofsky score below 70, pregnancy, or breast-feeding. Patients were followed until July 2011.

The study was approved by the Institutional Review Board of the Radboud University Nijmegen Medical Centre. Written informed consent was obtained from all patients.

Imaging Protocol

Preoperative T1-weighted MR images (3-dimensional rapid gradient echo; resolution, 1 × 1 × 1 mm; repetition time, 2,300 ms; inversion time, 1,100 ms; echo time, 4.71 ms) were obtained on a 3-T whole-body MRI system (TIM TRIO; Siemens), before and after contrast administration (0.1 mmol/kg bolus, 0.5 mM gadoteric acid [Dotarem; Guerbet]). The contrast-enhanced tumor volume (T1-ce) was manually delineated using the Pinnacle^3 radiotherapy treatment planning system (Philips) by subtracting the precontrast hyperintense volume of the tumor from the contrast-enhanced volume.

Patients underwent a preoperative ^{18}F-FLT PET/CT scan at most 3 d before surgery, with the exception of 2 patients (5 and 11 d). ^{18}F-FLT was obtained from the Department of Nuclear Medicine and PET Research, VU Medical Centre, Amsterdam, The Netherlands. Synthesis was performed as described previously (*16,17*). ^{18}F-FLT PET and CT images were acquired on a hybrid PET/CT scanner (Biograph; Siemens). Emission images of the head were recorded 60 min after intravenous injection of ^{18}F-FLT, with a median activity of 221 MBq (range, 108–277 MBq), for 10 min in 3-dimensional mode and reconstructed using the ordered-subset implementations iterative algorithm (4 iterations, 16 subsets, and 5-mm 3-dimensional gaussian filter). In addition, low-dose CT images (40 mAs, 130 kV) were acquired for anatomic correlation and attenuation-correction purposes. PET, CT, and MRI scans were coregistered and fused with software developed in-house.

The SUV_{max} of all tumors was derived from the coregistered ^{18}F-FLT PET/CT on the Pinnacle^3 radiotherapy planning system. The SUV_{max} was defined as the mean SUV of the hottest voxel of the tumor and its 8 surrounding voxels in a transversal slice (0.01 cm^3). Three different segmentation methods for estimating the PV were applied using Pinnacle^3 scripts developed in-house. The 50% isocontour of the SUV_{max} was used as a fixed lower threshold for calculating the proliferative volume $PV_{50\%}$. The signal-to-background ratio (SBR) as an adaptive threshold delineation method for calculating the proliferative volume PV_{SBR} has been described in detail by Schinagl et al. (*18*) and Daisne et al. (*19*). In brief, the threshold was derived from the following formula: threshold = a + b × 1/SBR, in which the parameters a and b are scanner-specific variables determined by a phantom experiment (*18,19*). The iterative background-subtracted relative threshold level (RTL) method was described in detail by van Dalen (*20*). In brief, to get a first volume estimate, the RTL of 50% was initially used. This volume was converted to an average diameter via $D = (V \times 6/\pi)^{1/3}$. The appropriate RTL for this diameter was calculated, and this process was iterated until the change of the

TABLE 2
SUV_{max}, PVs, and Enhanced T1 Tumor Volumes for Different Patients

Patient no.	SUV_{max}	$PV_{50\%}$ (cm^3)	PV_{SBR} (cm^3)	PV_{RTL} (cm^3)	T1-ce (cm^3)
1	1.54	18.6	11.5	9.7	9.6
2	3.76	30.5	42.8	34.0	10.3
3	2.36	5.6	10.0	8.0	5.8
4	0.67	24.3	7.3	6.9	12.1
5	1.38	25.0	34.3	26.5	13.1
6	1.76	9.1	11.8	9.5	8.2
7	0.67	3.0	5.1	4.2	4.1
8	1.75	15.1	17.9	15.3	9.6
9	3.54	16.4	27.8	19.7	53.5
10	1.12	19.5	20.3	16.3	6.2
11	1.75	7.5	8.2	7.2	6.4
12	1.26	6.1	7.4	6.6	5.8
13	0.92	1.4	1.1	1.1	0.5
14	0.90	5.8	3.2	9.6	7.8
15	1.06	7.6	8.0	7.0	3.8
16	1.06	7.5	9.2	6.9	1.2
17	1.05	44.1	32.7	25.8	30.8
18	0.72	10.3	8.6	7.8	2.9
19	2.08	7.2	12.3	9.5	12.8
20	0.74	28.8	18.8	17.7	4.3
21	1.39	28.4	53.1	33.1	20.5
22	3.48	18.4	29.6	22.1	21.7
23	2.59	5.6	11.3	8.3	13.6
24	3.10	16.5	38.0	22.0	21.6
25	2.33	17.2	27.8	22.1	25.0
26	0.60	17.5	12.8	10.4	4.3
Mean	1.68	15.3	18.1	14.1	12.1
95% confidence interval	1.29–2.06	11.1–19.4	12.7–23.6	10.5–17.8	7.5–16.7
Median	1.39	15.7	12.0	9.7	8.9
SD	0.96	10.3	13.5	9.0	11.4

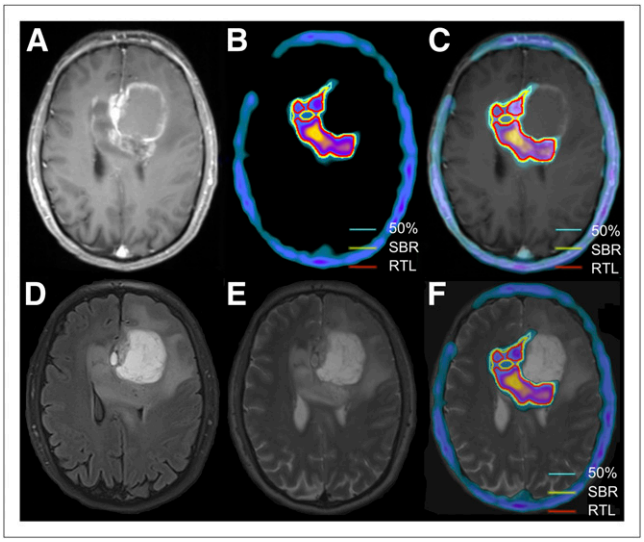

FIGURE 1. (A) T1-weighted MR image after contrast, showing left frontal ring-enhanced glioblastoma tumor with infiltration via corpus callosum to right side. (B) ^{18}F-FLT PET image with different segmented PVs. (C) Fused ^{18}F-FLT PET and T1-weighted MR image after contrast. (D) Fluid-attenuated inversion recovery MR image. (E) T2-weighted MR image. (F) Fused ^{18}F-FLT PET and T2-weighted MR image, showing most active localization of tumor in infiltrative part. 50% = PV of tumor based on 50% isocontour of SUV_{max}.

RTL was less than 1%. The volume calculated with this optimal RTL was used as the proliferative RTL volume PV_{RTL}. For the background activity, a volume of 0.65 cm^3 of normal-appearing tissue at the contralateral hemisphere—or in the case of a midline tumor, the contrafrontal or occipital hemisphere—was used.

For determining the variability of the segmentation methods, the mean and SD of the 3 different segmented PVs were calculated for each patient. The SD of the different segmented volumes was plotted against the mean of the different segmented volumes

Statistics

The Cox proportional hazards regression model (univariate Cox regression) with a backward likelihood ratio was used to assess the significance on OS of the covariates sex, age at operation, operation type (biopsy or resection), Karnofsky score at the time of surgery, the preoperative T1-ce volume, the SUV_{max}, and the different PVs. The significant covariates were used for multivariate regression with backward likelihood ratio. With receiver-operating-characteristic (ROC) curve analysis, we identified the threshold of the various PVs for patients with longer OS. Kaplan–Meier analysis with a log-rank statistical test was used to test the power of ^{18}F-FLT PET for predicting OS. All statistical analyses were performed with SPSS (version 16.0; IBM) for Windows (Microsoft).

RESULTS

Twenty-six patients (mean age, 52 y; age range, 35–67 y; 20 men, 6 women) were included in the study. Detailed patient characteristics are provided in Table 1. Tumor debulking was performed in 17 patients (4 gross total, 13 partial debulking), and in 9 patients the diagnosis was made using biopsy results. Most patients (n = 22) were diagnosed with glioblastoma. In the other patients, the diagnosis was anaplastic oligodendroglioma (ODIII; n = 2), anaplastic ependymoma (EIII; n = 1), and anaplastic astrocytoma (AIII; n = 1). Three patients had prior surgery because of a lower-grade tumor at respective intervals of half a year (diagnosis, grade II astrocytoma), 4 y (diagnosis, AIII), and 6 y (diagnosis, grade II oligodendroglioma) before. Two of these patients received prior EBRT. After the operation, all patients diagnosed with glioblastoma without previous treatment were treated with adjuvant EBRT and temozolomide chemotherapy conforming to the Stupp schedule (*1*), with the exception of 2 eligible patients (one patient refused adjuvant treatment, and the other had chronic lymphocytic leukemia and therefore received only EBRT). The patients diagnosed with glioblastoma and previously irradiated were treated with adjuvant temozolomide chemotherapy only. Patients with an ODIII were treated with EBRT after surgical resection. The patients with an AIII and EIII were first treated with EBRT and later adjuvant temozolomide chemotherapy. Eight patients underwent a second surgery, and 3 patients (all glioblastoma) received dendritic cell therapy after a second surgery. The median OS was 397 d (95% confidence interval, 204–577; range, 51–1379 d), and 19 patients died during the follow-up period (Table 1).

As shown in Table 2 and exemplified by Figure 1, in 18 patients (69%) the PV_{SBR} was the largest volume, compared with the PV_{RTL}, $PV_{50\%}$, and T1-ce volume (Wilcoxon signed rank test: $P < 0.001$, $P = 0.09$, and $P = 0.003$, respectively). Furthermore, the variability between the various methods for calculating the PV increased with increasing PV (Fig. 2).

The T1-ce, SUV_{max}, and PVs were independent significant predictors of survival in a univariate Cox regression model, and multivariate Cox regression showed significance only for the PV_{SBR} (Table 3). ROC analysis resulted in a volume threshold for the PV_{SBR} of 11.4 cm^3 (area

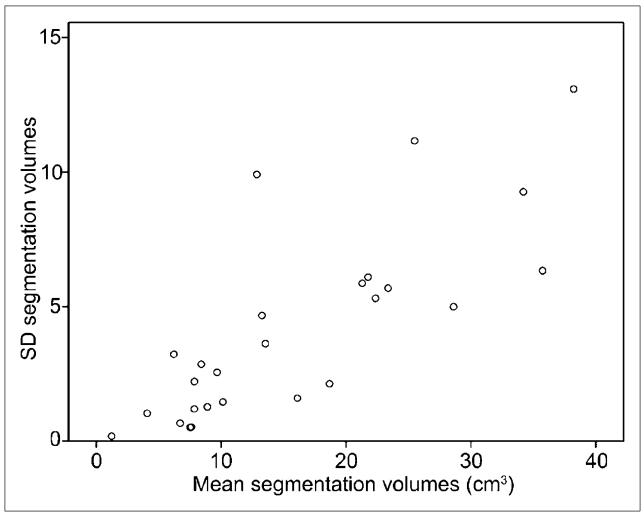

FIGURE 2. Correlation between tumor volume and variability between different segmented volumes. SDs between different segmented volumes are plotted against means of different segmented volumes, showing increasing SD with increasing volume.

TABLE 3
Cox Regression Results

Analysis	Covariate	Significance	Hazard ratio	95% confidence interval
Univariate Cox regression	Karnofsky	0.114	0.966	0.926–1.008
	Age at operation	0.55	1.043	0.999–1.090
	Sex	0.133	0.388	0.113–1.336
	Operation type	0.958	1.025	0.407–2.583
	SUV_{max}	0.021	1.863	1.099–3.159
	$PV_{50\%}$	0.047	1.050	1.001–1.102
	PV_{SBR}	0.002	1.061	1.022–1.101
	PV_{RTL}	0.007	1.076	1.020–1.135
	T1-ce	0.019	1.045	1.007–1.085
Multivariate Cox regression, backward likelihood ratio	PV_{SBR}	0.002	1.061	1.022–1.101

under the curve, 85%; sensitivity, 70%; specificity, 83%). Kaplan–Meier analyses showed a significant discrimination between short and long survival ($P = 0.024$; log rank) for this threshold (Fig. 3A). A volume of less than 7.4 cm^3 PV_{SBR} was indicative of long-term survival ($P = 0.004$; log rank; Fig. 3B), and a PV_{SBR} of more than 24 cm^3 indicated a poor prognosis with no survivors beyond 2 y ($P = 0.01$; log rank; Fig. 3C). ROC analysis was not significant for T1-ce, SUV_{max}, and $PV_{50\%}$. ROC analysis for PV_{RTL} resulted in a volume threshold of 8.9 cm^3 (area under the curve, 78%; sensitivity, 70%; specificity, 67%). However, Kaplan–Meier analysis was not significant for this volume threshold.

DISCUSSION

In this study, we demonstrate that the PV of high-grade glioma calculated from a single pretherapy ^{18}F-FLT PET/CT scan predicts OS of high-grade glioma patients. For this purpose, the PV_{SBR} proved to be the method of choice. The T1-ce, SUV_{max}, and other PVs were also independent significant predictors of the OS, but PV_{RTL} failed to identify a clear threshold value, and ROC analysis for T1-ce, SUV_{max}, and $PV_{50\%}$ was not significant.

Earlier publications have shown that quantitative analysis of ^{18}F-FLT PET may also discriminate recurrent tumor from posttreatment radionecrosis (*21*). Furthermore, the potential of sequential ^{18}F-FLT PET has been reported for early outcome predictions of systemic therapy in patients with recurrent malignant glioma (*22,23*).

For quantitative analysis of PET, mainly the SUV is calculated or more sophisticated kinetic models are used (*11,23,24*). The mean SUV of the tumor is often calculated after manual delineation of the tumor. The major disadvantages of this approach are the operator dependency and the susceptibility to window-level settings. The SUV_{max} is not operator-dependent but is subject to variability in data acquisition and processing (*18,25*). With automated methods, these confounding factors have less influence on the results. User-independent segmentation algorithms for calculating the PV are much less prone to such errors. Segmentation with the RTL method incorporates the size of the tumor into the algorithm, is independent of the SBR, and inherently assumes spheroid tumor volumes (*20*). This method might be the better solution for solid tumors. However, high-grade gliomas are heterogeneous and may present as multifocal

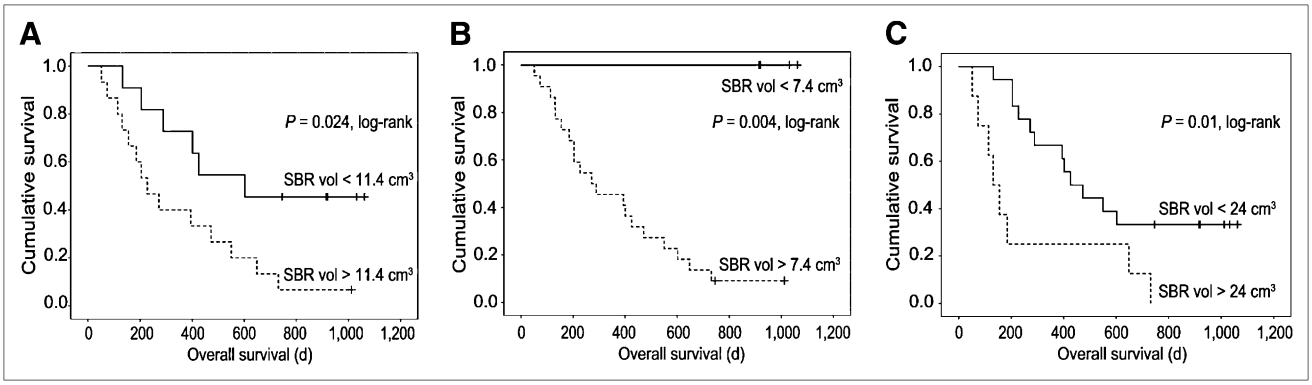

FIGURE 3. Kaplan–Meier estimates of OS using PV_{SBR}. (A) PV_{SBR} of 11.4 cm^3 significantly differentiates 2 groups of patients, with sensitivity of 70%, specificity of 83%, and area under the curve of 85%. (B) PV_{SBR} of less than 7.4 cm^3 indicates relatively long-term survival (>4 y). (C) PV_{SBR} of more than 24 cm^3 indicates poor prognosis, with no patient surviving more than 2 y.

lesions. Therefore, the RTL algorithm might be less suitable for the evaluation of multiple lesions than the SBR method. Because of these multifocal and heterogeneous aspects of gliomas, a proliferative volume appears more representative than the SUV_{max} for predicting the OS. Whereas the SUV_{max} is the representation of 1 point in the tumor, the proliferative volume takes into account both the degree of proliferation and the volume, which expresses enhanced proliferation.

One of the limitations of ^{18}F-FLT might be that a disruption of the blood–brain barrier is required for tumor targeting (*9*). Especially for low-grade gliomas, this requirement can be a restricting factor. For this reason, we selected only high-grade gliomas, in which the blood–brain barrier is always disrupted. Remarkably, we observed that the intracerebral uptake of ^{18}F-FLT was not limited to areas of contrast enhancement as seen on MRI and in fact exceeded the area of contrast enhancement on the MRI in most cases. This finding implies that the uptake of ^{18}F-FLT is not limited to a damaged blood–brain barrier as defined by contrast enhancement on MRI. One explanation might be the difference in resolution between PET and MRI. In areas of necrosis, in which mostly a ring of contrast enhancement is found, the uptake of ^{18}F-FLT in this ring is mostly high and the segmented volume is expanded partly inside the necrotic area. Another possible explanation is that the size of gadoteric acid contrast is larger than ^{18}F-FLT. ^{18}F-FLT uptake might therefore already occur in an area of earlier and less severe blood–brain barrier damage. This area might be associated with the relative cerebral blood volume (rCBV), which has a stronger predictive value than conventional MRI in cerebral glioma (*26,27*). In low-grade glioma, the rCBV might reflect better the histopathology of the tumor (*26*). Weber et al. showed that in 75% of brain glioma cases, the ^{18}F-FLT uptake is correlated to the rCBV (*28*). A limitation of ^{18}F-FLT can be the ^{18}F-FLT uptake in the bone marrow of the skull, which might interfere with calculation of the tumor volume. Another limitation of our study might be the different treatments of the patients. Although almost all patients received radiotherapy and chemotherapy, not all patients underwent a second operation. Additionally, 3 patients had previously undergone surgery, and of those, 2 received adjuvant radiotherapy. Whether and how pretreatment influenced ^{18}F-FLT targeting cannot be established, but pretreatment apparently did not negatively affect the correlation of the PV and patient survival. However, the interpretation of the statistical analysis should be done with caution because of the limited number of patients relative to the number of variables.

The use of static rather than dynamic PET obviously prevents kinetic modeling. Because the Ki-67 index correlates best with the Ki derived from dynamic PET, static scanning may be considered a limitation of our study (*13,14*). Wardak et al. reported a better predictive value with a combination of kinetic parameters for the OS and progression-free survival than with single kinetic parameters and the SUV (*29*). However, this is probably not a major issue in imaging glioma, because others also showed good correlation of SUV_{max} with the Ki-67 index (*30*). Additionally, calculation of the PV does not require kinetic modeling.

CONCLUSION

We have shown that a single pretreatment ^{18}F-FLT PET/CT and subsequent calculation of the PV predicts OS in high-grade glioma, also providing thresholds that separate patients with long survival from those with a poor prognosis. The PV_{SBR} method provides a simple, user-independent, clinically easily performed method for assessing the volume of the proliferative part of the tumor. These are important factors for implementing this technique into neurooncology clinical practice. The PV_{SBR} might assist in clinical decision making on the choice of treatment. Furthermore, our findings may serve as a basis for future studies in which the proliferative part of tumors is subject to different therapeutic interventions (surgery, radiosurgery, stereotactic radiotherapy, or systemic targeted therapy). Whether the PV_{SBR} can be used for monitoring and adjusting treatment of glioma is a question that will have to be resolved in future studies.

DISCLOSURE STATEMENT

The costs of publication of this article were defrayed in part by the payment of page charges. Therefore, and solely to indicate this fact, this article is hereby marked "advertisement" in accordance with 18 USC section 1734.

ACKNOWLEDGMENTS

The study was supported in part by an unrestricted grant from Schering Plough. No other potential conflict of interest relevant to this article was reported.

REFERENCES

1. Stupp R, Mason WP, van den Bent MJ, et al. Radiotherapy plus concomitant and adjuvant temozolomide for glioblastoma. *N Engl J Med.* 2005;352:987–996.
2. Stummer W, Pichlmeier U, Meinel T, Wiestler OD, Zanella F, Reulen HJ. Fluorescence-guided surgery with 5-aminolevulinic acid for resection of malignant glioma: a randomised controlled multicentre phase III trial. *Lancet Oncol.* 2006;7:392–401.
3. Claes A, Idema AJ, Wesseling P. Diffuse glioma growth: a guerilla war. *Acta Neuropathol.* 2007;114:443–458.
4. Smith JS, Chang EF, Lamborn KR, et al. Role of extent of resection in the long-term outcome of low-grade hemispheric gliomas. *J Clin Oncol.* 2008;26:1338–1345.
5. Ewelt C, Goeppert M, Rapp M, Steiger HJ, Stummer W, Sabel M. Glioblastoma multiforme of the elderly: the prognostic effect of resection on survival. *J Neurooncol.* 2011;103:611–618.
6. Gorlia T, van den Bent MJ, Hegi ME, et al. Nomograms for predicting survival of patients with newly diagnosed glioblastoma: prognostic factor analysis of EORTC and NCIC trial 26981-22981/CE.3. *Lancet Oncol.* 2008;9:29–38.
7. Widhalm G, Krssak M, Minchev G, et al. Value of ^{1}H-magnetic resonance spectroscopy chemical shift imaging for detection of anaplastic foci in diffusely infiltrating gliomas with non-significant contrast-enhancement. *J Neurol Neurosurg Psychiatry.* 2011;82:512–520.

8. Shields AF, Grierson JR, Dohmen BM, et al. Imaging proliferation in vivo with [F-18]FLT and positron emission tomography. *Nat Med.* 1998;4:1334–1336.
9. Barwick T, Bencherif B, Mountz JM, Avril N. Molecular PET and PET/CT imaging of tumour cell proliferation using F-18 fluoro-L-thymidine: a comprehensive evaluation. *Nucl Med Commun.* 2009;30:908–917.
10. Kong XB, Zhu QY, Vidal PM, et al. Comparisons of anti-human immunodeficiency virus activities, cellular transport, and plasma and intracellular pharmacokinetics of 3′-fluoro-3′-deoxythymidine and 3′-azido-3′-deoxythymidine. *Antimicrob Agents Chemother.* 1992;36:808–818.
11. Chen W, Cloughesy T, Kamdar N, et al. Imaging proliferation in brain tumors with ^{18}F-FLT PET: comparison with ^{18}F-FDG. *J Nucl Med.* 2005;46:945–952.
12. Backes H, Ullrich R, Neumaier B, Kracht L, Wienhard K, Jacobs AH. Noninvasive quantification of ^{18}F-FLT human brain PET for the assessment of tumour proliferation in patients with high-grade glioma. *Eur J Nucl Med Mol Imaging.* 2009;36:1960–1967.
13. Price SJ, Fryer TD, Cleij MC, et al. Imaging regional variation of cellular proliferation in gliomas using 3′-deoxy-3′-[^{18}F]fluorothymidine positron-emission tomography: an image-guided biopsy study. *Clin Radiol.* 2009;64:52–63.
14. Ullrich R, Backes H, Li H, et al. Glioma proliferation as assessed by 3′-fluoro-3′-deoxy-L-thymidine positron emission tomography in patients with newly diagnosed high-grade glioma. *Clin Cancer Res.* 2008;14:2049–2055.
15. Muzi M, Spence AM, O'Sullivan F, et al. Kinetic analysis of 3′-deoxy-3′-^{18}F-fluorothymidine in patients with gliomas. *J Nucl Med.* 2006;47:1612–1621.
16. Machulla HJ, Blocher A, Kuntzsch M, Piert M, Wei R, Grierson JR. Simplified labeling approach for synthesizing 3′-deoxy-3′-[^{18}F]fluorothymidine ([^{18}F]FLT). *J Radioanal Nucl Chem.* 2000;243:843–846.
17. Troost EG, Vogel WV, Merkx MA, et al. ^{18}F-FLT PET does not discriminate between reactive and metastatic lymph nodes in primary head and neck cancer patients. *J Nucl Med.* 2007;48:726–735.
18. Schinagl DA, Vogel WV, Hoffmann AL, van Dalen JA, Oyen WJ, Kaanders JH. Comparison of five segmentation tools for ^{18}F-fluoro-deoxy-glucose-positron emission tomography-based target volume definition in head and neck cancer. *Int J Radiat Oncol Biol Phys.* 2007;69:1282–1289.
19. Daisne JF, Sibomana M, Bol A, Doumont T, Lonneux M, Gregoire V. Tri-dimensional automatic segmentation of PET volumes based on measured source-to-background ratios: influence of reconstruction algorithms. *Radiother Oncol.* 2003;69:247–250.
20. van Dalen JA, Hoffmann AL, Dicken V, et al. A novel iterative method for lesion delineation and volumetric quantification with FDG PET. *Nucl Med Commun.* 2007;28:485–493.
21. Spence AM, Muzi M, Link JM, et al. NCI-sponsored trial for the evaluation of safety and preliminary efficacy of 3′-deoxy-3′-[^{18}F]fluorothymidine (FLT) as a marker of proliferation in patients with recurrent gliomas: preliminary efficacy studies. *Mol Imaging Biol.* 2009;11:343–355.
22. Schwarzenberg J, Czernin J, Cloughesy TF, et al. 3′-deoxy-3′-^{18}F-fluorothymidine PET and MRI for early survival predictions in patients with recurrent malignant glioma treated with bevacizumab. *J Nucl Med.* 2012;53:29–36.
23. Schiepers C, Dahlbom M, Chen W, et al. Kinetics of 3′-deoxy-3′-^{18}F-fluorothymidine during treatment monitoring of recurrent high-grade glioma. *J Nucl Med.* 2010;51:720–727.
24. Chen W, Delaloye S, Silverman DH, et al. Predicting treatment response of malignant gliomas to bevacizumab and irinotecan by imaging proliferation with [^{18}F] fluorothymidine positron emission tomography: a pilot study. *J Clin Oncol.* 2007;25:4714–4721.
25. Hatt M, Cheze-Le Rest C, Aboagye EO, et al. Reproducibility of ^{18}F-FDG and 3′-deoxy-3′-^{18}F-fluorothymidine PET tumor volume measurements. *J Nucl Med.* 2010;51:1368–1376.
26. Law M, Yang S, Wang H, et al. Glioma grading: sensitivity, specificity, and predictive values of perfusion MR imaging and proton MR spectroscopic imaging compared with conventional MR imaging. *AJNR.* 2003;24:1989–1998.
27. Law M, Oh S, Johnson G, et al. Perfusion magnetic resonance imaging predicts patient outcome as an adjunct to histopathology: a second reference standard in the surgical and nonsurgical treatment of low-grade gliomas. *Neurosurgery.* 2006;58:1099–1107.
28. Weber MA, Henze M, Tuttenberg J, et al. Biopsy targeting gliomas: do functional imaging techniques identify similar target areas? *Invest Radiol.* 2010;45:755–768.
29. Wardak M, Schiepers C, Dahlbom M, et al. Discriminant analysis of ^{18}F-fluorothymidine kinetic parameters to predict survival in patients with recurrent high-grade glioma. *Clin Cancer Res.* 2011;17:6553–6562.
30. Saga T, Kawashima H, Araki N, et al. Evaluation of primary brain tumors with FLT-PET: usefulness and limitations. *Clin Nucl Med.* 2006;31:774–780.